DIFFUSION IN CONFINEMENT: DISTINCT KINETIC PATHWAYS TO AGGREGATE GROWTH

C. Chimerel, ***Faculty of Engineering, "Constantin Brancusi" University of Targu Jiu, Targu Jiu,*** **ROMANIA**

ABSTRACT: Spatial confinement critically modulates diffusion kinetics in diverse biological and synthetic microenvironments, including cellular interiors, microreactors, and emulsion droplets. The interplay between boundary constraints and interparticle interactions generates complex, evolving system dynamics. Here, we present a Python-based computational framework designed to simulate the Brownian dynamics of finite-sized, non-overlapping particles confined within a circular geometry. The model incorporates hard-sphere exclusion and stochastic trajectories, coupled with a probabilistic collision-fusion mechanism. To investigate perturbations in system equilibrium, we analyze the dynamic evolution of the system under the influence of a "super-absorber"—a single localized entity possessing an elevated fusion probability—and compare its behavior against a baseline regime governed by uniform collision-fusion kinetics.

KEY WORDS: diffusion, equilibrium, confinement, coalescence, Brownian dynamics.

1. INTRODUCTION. The dynamics of phase separation, aggregation, and nucleation in confined geometries play an important role across widely disparate fields of natural science, from the formation of atmospheric aerosols to the liquid-liquid phase separation in cells [1, 2]. At the heart of these phenomena is the competition between diffusion-driven mass flux and discrete coalescence events. While the thermodynamic endpoints of closed-system aggregation are well-defined—inevitably resulting in complete phase separation or a single macroscopic sink—the kinetic pathways leading to these states are highly complex and heavily dependent on localized interaction probabilities [3].

Historically, the kinetics of bulk particle coalescence have been modeled using the Smoluchowski coagulation equation, which describes the time evolution of particle size distributions undergoing Brownian motion and merging upon collision [4]. However, real-world systems often exhibit a hybrid behavior: a "mobile phase" of interacting, diffusing particles competing with fixed "nucleation sites". In such systems, the diffusion coefficient of the mobile -diffusion driven - phase is not constant but scales inversely with the hydrodynamic radius of the aggregated particles, in accordance with the Stokes-Einstein relation ($D \propto 1/r$) [5].

This size-dependent mobility introduces a non-trivial feedback loop into the system's growth kinetics. As mobile particles coalesce in the bulk phase, their diffusion slows dramatically. Consequently, the rate at which mass is delivered to fixed macroscopic boundaries—such as cellular receptors, synthetic thin-film defects, or engineered nanomaterial surfaces—is fundamentally altered. A critical, yet underexplored, question is how the probability of mobile-mobile coalescence versus mobile-fixed absorption dictates the structural evolution and growth rate of the macroscopic sink in a confined geometry. Does rapid pre-assembly in the bulk phase accelerate ultimate deposition, or does it starve the fixed site by generating sluggish, massive intermediates?

To address this, we present a computational model utilizing discrete Brownian dynamics to simulate mass-conserving aggregation within a 2D confined space. By parameterizing the fusion probability of mobile-mobile collisions (P_{merge}^{mobile}) independently from mobile-fixed collisions (P_{merge}^{nuc}), we map the kinetic regimes that govern nucleation site growth. We demonstrate that altering the mobile fusion probability shifts the nucleation growth curve from a smooth, continuous mass influx—driven by a highly mobile "gas" of small particles—to a stochastic, step-wise growth pattern characterized by rare but massive delivery events.

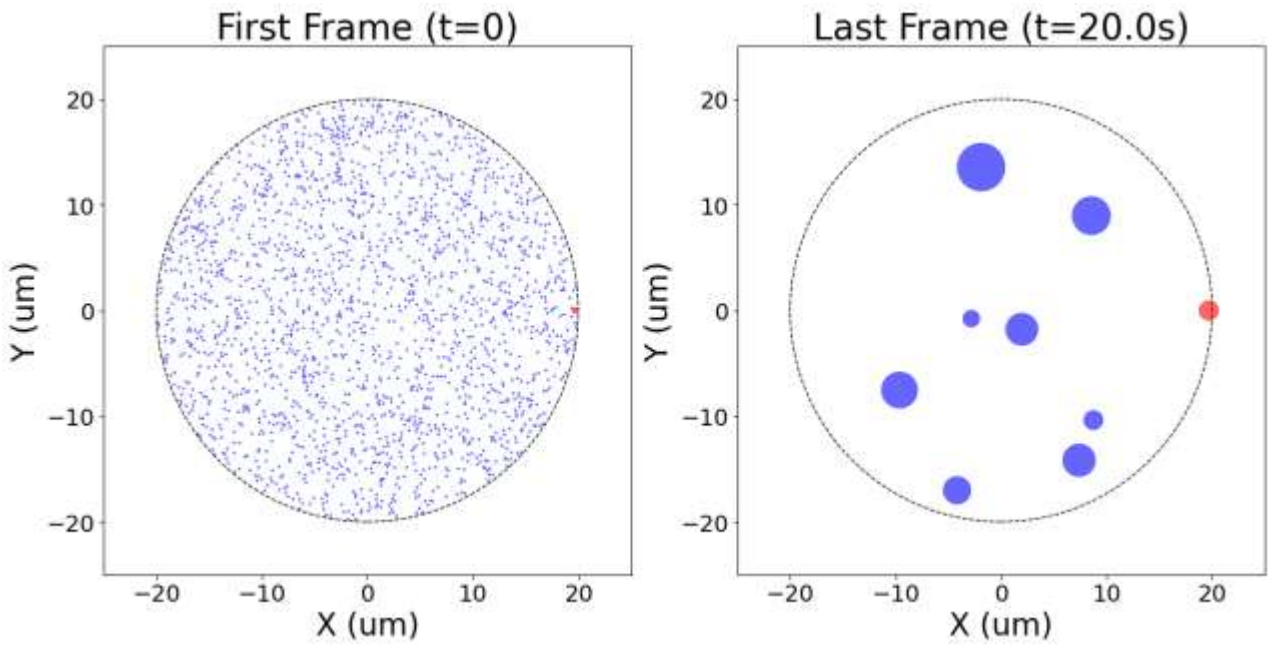

Figure 1. Simulation of particle diffusion and coalescence in a confined circular geometry. The left panel shows the initial particle distribution at t=0s, and the right panel presents a snapshot of the system after 20 seconds. The fusion probability is set to P_{merge}^{mobile} =P_{merge}^{nuc}.=0.5 for both mobile-mobile particle collisions and collisions with the fixed nucleation site.

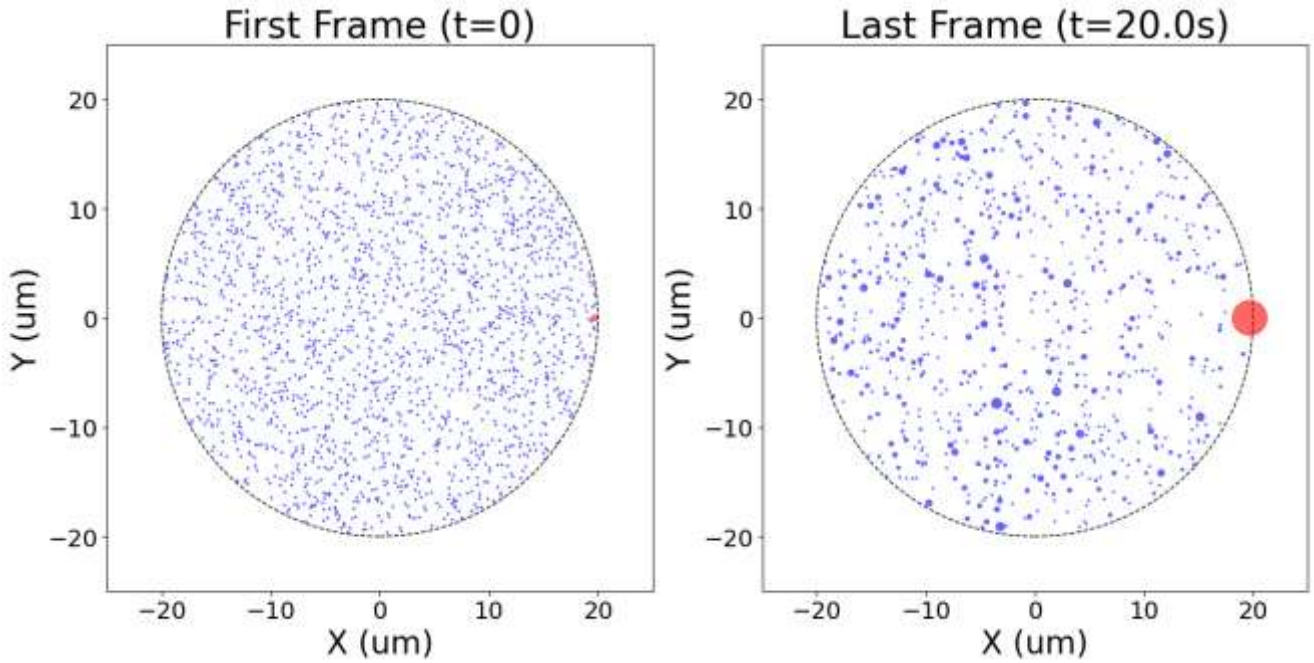

Figure 2. Simulation of particle diffusion and coalescence in a confined circular geometry. The left panel shows the initial particle distribution at t=0s, and the right panel presents a snapshot of the system after 20 seconds. The fusion probability is set to P_{merge}^{mobile} =0.005 for the mobile-mobile particle collisions and to P_{merge}^{nuc}=0.5 for the collisions with the fixed nucleation site.

2. METHODS. System Initialization and Domain Description. Two-dimensional Brownian dynamics simulations were developed to model colloidal diffusion and coalescence in an aqueous medium at room temperature. The simulation environment consisted of a circular confinement domain with a diameter of 40 micrometres,

incorporating a single fixed nucleation site on the surface. The system was initialized with mobile colloidal particles (initial diameter = 0.2 μm) to achieve a target area fraction of 10%. Initial spatial coordinates were generated using a random sequential adsorption (RSA) algorithm; particles were iteratively and randomly placed, with no overlap.

Brownian Dynamics and Boundary Conditions. Particle trajectories were propagated using a discrete-time random walk, where trial displacements were sampled from a Gaussian distribution. In accordance with the Stokes-Einstein relation, the diffusion coefficient D for each aggregate was scaled inversely with its radius ($D \propto 1/r$), yielding reduced mobility for larger coalesced structures. The fixed nucleation site was assigned a diffusion coefficient of zero. The circular confinement was modelled utilizing hard-wall boundary conditions. During the integration step, any calculated displacement that caused a mobile particle's radius to intersect or cross the simulation boundary was entirely rejected, nullifying the step for that specific temporal frame.

Collision Detection and Coalescence Kinetics. To computationally manage the particle environment (5% filling fraction) which equates almost 2000 particles, spatial proximity queries were optimized using a K-Dimensional Tree algorithm (scipy.spatial.cKDTree). Interparticle overlap was strictly forbidden. Upon collision detection, a stochastic evaluation determined the interaction outcome based on pre-defined probabilities for mobile-mobile and mobile-nucleation site events. If the evaluation dictated a reflection, the involved particles reverted to their pre-step coordinates (step cancellation). If coalescence was dictated, two-dimensional mass (area) was conserved such that the newly formed aggregate's radius was calculated as $r_{new} = \text{sqrt}(r_1^2 + r_2^2)$. The spatial coordinates of the new aggregate were assigned to the area-weighted centre of mass of the parent particles; however, if the coalescence involved the nucleation site, the new aggregate inherited the exact coordinates of the fixed site.

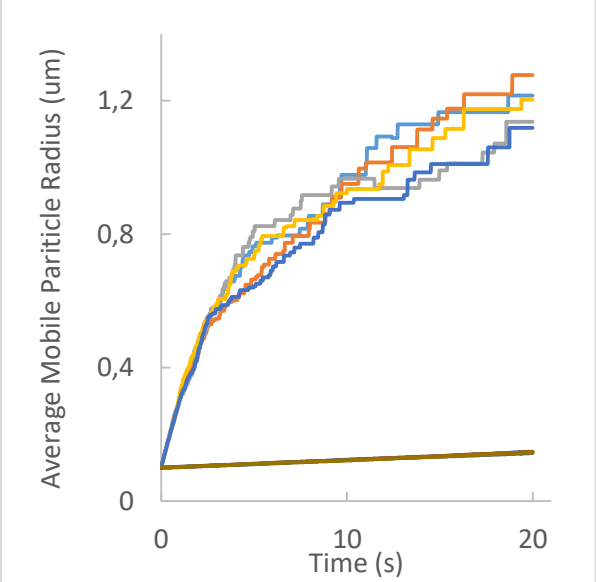

Figure 3. Time evolution of the average mobile particle radius. ***Top curves*** show simulations where the fusion probability is set to $P_{merge}^{mobile}=P_{merge}^{nuc}=0.5$. ***Bottom curves*** show simulations where $P_{merge}^{mobile}=0.005$ while $P_{merge}^{nuc}=0.5$.

Multiparticle Crowding and Cascading Overlaps. To account for the high packing fraction, an iterative collision resolution protocol was implemented to handle cascading overlaps. If a newly coalesced aggregate subsequently overlapped with pre-existing adjacent particles in the same time step, secondary collision events were immediately evaluated. If secondary coalescence was rejected (reflection), the excluded volume condition was rigorously enforced by displacing the smaller particle to the nearest available, non-overlapping spatial coordinate in direct contact with the surface of the larger aggregate.

The temporal evolution of the system was simulated over 2000 steps using a constant discrete time step of $\Delta t=0.01$ s. This temporal resolution was selected to ensure accurate representation of the stochastic diffusion trajectories while maintaining computational efficiency. The mobility of the particles was modelled using a size-dependent diffusion coefficient, approximating the Stokes-Einstein relation. A base diffusion coefficient of $D_0=1.0\ \mu m^2/s$ was assigned to particles with a reference radius of 1 μm. For all mobile particles and subsequent aggregates, the effective diffusion coefficient (D) was scaled inversely with the particle radius (r) according to $D=D_0/r$, ensuring that larger coalesced clusters exhibited realistically reduced mobility. During the preparation of this work, the author(s) used Google Gemini to assist in writing Python code for the simulations and to refine the academic language of the manuscript. After using this tool/service, the author(s) reviewed and edited the content as needed and take(s) full responsibility for the accuracy and integrity of the final publication.

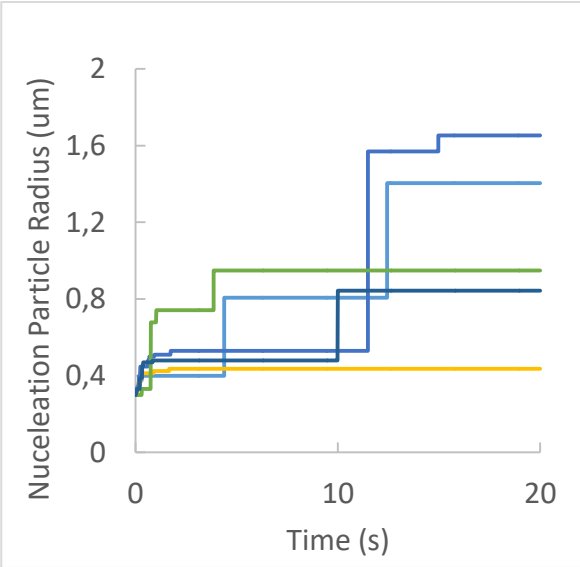

Figure 4. Time evolution of the average nucleation particle radius when the $\mathbf{P_{merge}^{mobile}=P_{merge}^{nuc}=0.5}$. A number of 5 independent simulations are displayed here.

3. RESULTS

We analysed the spatiotemporal evolution of colloidal particles (initial radius = 0.1 μm) confined within a 20 μm radius circular domain. A single, fixed nucleation site (initial radius = 0.3 μm) was seeded at the confinement boundary. Simulations were executed for a total temporal duration of 20 seconds. To investigate the effect of bulk particle interactions on boundary nucleation, the mobile-mobile particle coalescence probability was varied between 0.5 and 0.005, while the mobile-nucleation site coalescence probability was held constant at 0.5. Qualitative assessment of the final states (Figures 1 and 2) reveals distinct kinetic pathways governing aggregate growth. Under high bulk coalescence conditions (probability = 0.5, Figure 1), mobile particles undergo rapid fusion in the bulk phase, significantly increasing their mean radius, while the relative growth of the fixed nucleation site is hindered. Conversely, when bulk coalescence is suppressed (probability = 0.005, Figure 2), the mobile particles remain small and highly numerous. This suppression of bulk aggregation preserves high diffusive mobility within the domain, effectively redirecting the system's mass flux toward the confinement boundary and rendering the nucleation site the largest aggregate in the simulation. To substantiate these qualitative morphological differences, we proceed to quantitatively analyze the particle growth dynamics.

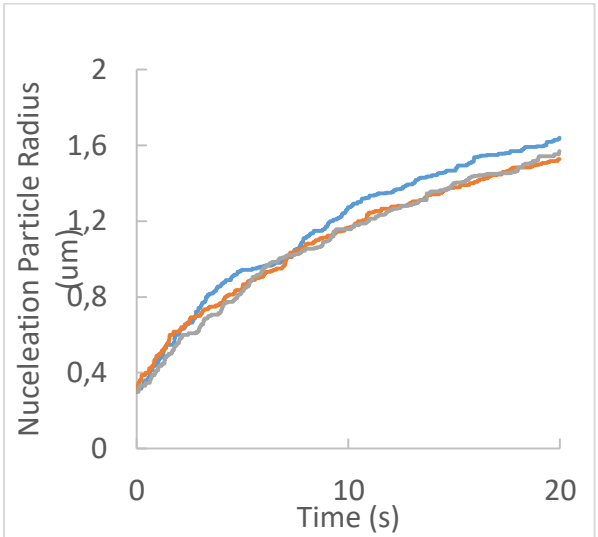

Figure 5. Time evolution of the average nucleation particle radius when the **P_{merge}^{mobile}=0.005 and the P_{merge}^{nuc}=0.5**. A number of 3 independent simulations are displayed here.

To further investigate this phenomenon, Figures 4 and 5 illustrate the temporal growth profiles of the nucleation site under the two distinct simulation conditions. We observe that, despite reducing the mobile-mobile coalescence probability P_{merge}^{mobile} by two orders of magnitude, the nucleation site continues to grow in both scenarios; however, the underlying growth kinetics differ dramatically. In Figure 4, the nucleation radius exhibits step-wise increases, a characteristic signature of infrequent, large-scale coalescence events. Conversely, Figure 5 demonstrates a continuous, smooth increase in the nucleation radius, indicative of a steady mass influx from smaller individual particles.

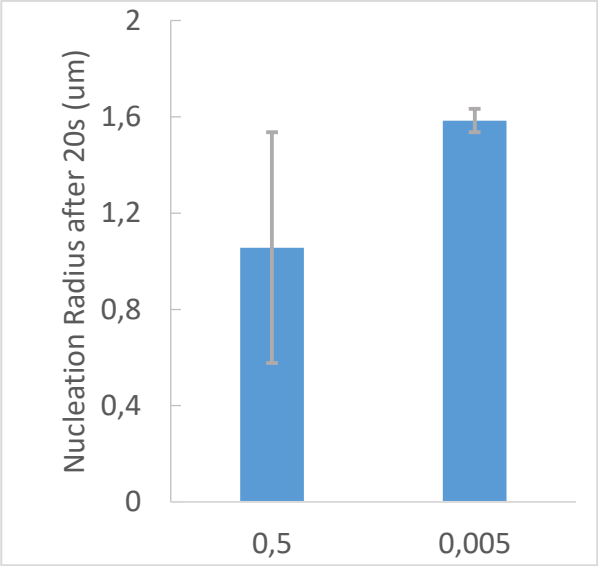

Figure 6. The average nucleation particle radius after 20 seconds of simulation when the mobile merge probability P_{merge}^{mobile} in the simulation is changed from 0.5 (N=5 repeats) to 0.005 (N=4 repeats).

Interestingly, Figure 6 demonstrates that after 20 seconds of simulation, the average final radius of the nucleation site is statistically equivalent (within experimental error) across both simulation conditions. However, the magnitude of the variance—represented by the error bars—reveals fundamentally different underlying growth mechanisms. The broad error bars observed under high bulk-coalescence conditions reflect a highly stochastic build-up process, characterized by rare but massive fusion events with large mobile aggregates. In contrast, the narrow error bars seen under restricted bulk-coalescence conditions are indicative of a continuous, diffusion-driven mass flux, where the nucleation site steadily and predictably accumulates mass through frequent interactions with small, highly mobile particles.

4. CONCLUSION

In conclusion, our simulations demonstrate that the kinetic pathway of localized aggregate growth is highly sensitive to the bulk coalescence probability of the system. By systematically varying the fusion probability among mobile particles while maintaining a constant interaction probability at a fixed nucleation site, we observed a fundamental shift in mass transport mechanisms. High bulk coalescence rates favor the rapid formation of large, slow-moving aggregates, leading to a highly stochastic, step-wise growth of the nucleation site governed by rare collision events. Conversely, suppressing bulk coalescence preserves the high diffusivity of a large population of small particles. This shifts the system into a continuous, diffusion-driven mass flux regime, enabling steady and predictable growth at the boundary. Interestingly, despite these divergent kinetic pathways—stochastic build-up versus continuous accumulation—the final average radius of the nucleation site was statistically equivalent over the simulated timeframe. These findings highlight that while the macroscopic mass transfer may eventually converge, the microscopic dynamics and variance governing the assembly process are

entirely distinct, which has significant implications for controlling phase separation and targeted aggregate growth in confined colloidal systems.

5. REFERENCES

[1] Seinfeld, J. H., & Pandis, S. N. Atmospheric Chemistry and Physics: From Air Pollution to Climate Change. John Wiley & Sons, 2016.
[2] Mangiarotti, A., & Dimova, R. Biomolecular condensates in contact with membranes. Annual Review of Biophysics, 53, 319-341, 2024.
[3] Lifshitz, I. M., & Slyozov, V. V. The kinetics of precipitation from supersaturated solid solutions. Journal of Physics and Chemistry of Solids, 19(1-2), 35-50, 1961.
[4] von Smoluchowski, M. Drei Vorträge über Diffusion, Brownsche Molekularbewegung und Koagulation von Kolloidteilchen. Physikalische Zeitschrift, 17, 557-585, 1916.
[5] Einstein, A. Über die von der molekularkinetischen Theorie der Wärme geforderte Bewegung von in ruhenden Flüssigkeiten suspendierten Teilchen. Annalen der Physik, 322(8), 549-560, 1905.